NASA/TM–2003–212408

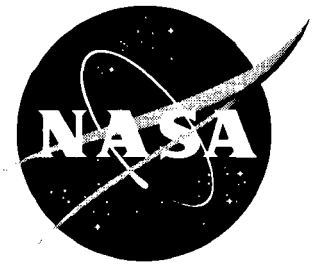

Profile Optimization Method for Robust Airfoil Shape Optimization in Viscous Flow

Wu Li
Langley Research Center, Hampton, Virginia

May 2003

The NASA STI Program Office ... in Profile

Since its founding, NASA has been dedicated to the advancement of aeronautics and space science. The NASA Scientific and Technical Information (STI) Program Office plays a key part in helping NASA maintain this important role.

The NASA STI Program Office is operated by Langley Research Center, the lead center for NASA's scientific and technical information. The NASA STI Program Office provides access to the NASA STI Database, the largest collection of aeronautical and space science STI in the world. The Program Office is also NASA's institutional mechanism for disseminating the results of its research and development activities. These results are published by NASA in the NASA STI Report Series, which includes the following report types:

- TECHNICAL PUBLICATION. Reports of completed research or a major significant phase of research that present the results of NASA programs and include extensive data or theoretical analysis. Includes compilations of significant scientific and technical data and information deemed to be of continuing reference value. NASA counterpart of peer-reviewed formal professional papers, but having less stringent limitations on manuscript length and extent of graphic presentations.
- TECHNICAL MEMORANDUM. Scientific and technical findings that are preliminary or of specialized interest, e.g., quick release reports, working papers, and bibliographies that contain minimal annotation. Does not contain extensive analysis.
- CONTRACTOR REPORT. Scientific and technical findings by NASA-sponsored contractors and grantees.
- CONFERENCE PUBLICATION. Collected papers from scientific and technical conferences, symposia, seminars, or other meetings sponsored or co-sponsored by NASA.
- SPECIAL PUBLICATION. Scientific, technical, or historical information from NASA programs, projects, and missions, often concerned with subjects having substantial public interest.
- TECHNICAL TRANSLATION. English-language translations of foreign scientific and technical material pertinent to NASA's mission.

Specialized services that complement the STI Program Office's diverse offerings include creating custom thesauri, building customized databases, organizing and publishing research results ... even providing videos.

For more information about the NASA STI Program Office, see the following:

- Access the NASA STI Program Home Page at ***http://www.sti.nasa.gov***
- E-mail your question via the Internet to help@sti.nasa.gov
- Fax your question to the NASA STI Help Desk at (301) 621-0134
- Phone the NASA STI Help Desk at (301) 621-0390
- Write to:
  NASA STI Help Desk
  NASA Center for AeroSpace Information
  7121 Standard Drive
  Hanover, MD 21076-1320

NASA/TM–2003–212408

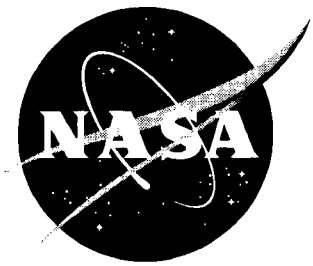

Profile Optimization Method for Robust Airfoil Shape Optimization in Viscous Flow

Wu Li
Langley Research Center, Hampton, Virginia

National Aeronautics and
Space Administration

Langley Research Center
Hampton, Virginia 23681–2199

May 2003

Acknowledgments

We would like to thank Eric Nielsen and Mark Chaffin for their assistance with using FUN2D to generate the simulation results.

Available from:

NASA Center for AeroSpace Information (CASI)
7121 Standard Drive
Hanover, MD 21076–1320
(301) 621–0390

National Technical Information Service (NTIS)
5285 Port Royal Road
Springfield, VA 22161–2171
(703) 605–6000

Abstract

Simulation results obtained by using FUN2D for robust airfoil shape optimization in transonic viscous flow are included to show the potential of the profile optimization method for generating fairly smooth optimal airfoils with no off-design performance degradation.

Nomenclature

c	chord length of airfoil
c_d	drag coefficient
$\frac{\partial c_d}{\partial D}$	gradient of c_d with respect to D
$\frac{\partial c_d}{\partial \alpha}$	derivative of c_d with respect to α
c_l	lift coefficient
$\frac{\partial c_l}{\partial D}$	gradient of c_l with respect to D
$\frac{\partial c_l}{\partial \alpha}$	derivative of c_l with respect to α
c_l^*	target lift coefficient
D	design vector
$E(\cdot)$	mean of random variable
$\mathcal{F}$	feasible set for the design vector D
M	free-stream Mach number
n	number of design variables
$p(M)$	probability density function of Mach number
r	number of design conditions
x, y	coordinates of points on plane
α	angle of attack
$\gamma_{\min}$	minimum rate of drag reduction at all design conditions
ΔD	change in design vector
$\delta_{k,i}$, ρ_k	scalars defining the trust region
$\sigma^2(\cdot)$	variance of random variable
Ω	a given Mach range
$\langle \cdot, \cdot \rangle$	inner product in Euclidean space

Subscripts and Superscripts

i	index for design condition
j	index for component of design vector
k	index for iteration or iterate

1 Introduction

This paper is an extension of reference 1, where the profile optimization method was proposed to resolve off-design performance degradation problems encountered by multipoint

optimization methods (ref. 2). Numerical simulation results given in reference 1, though very encouraging, were not representative of realistic airfoil shape optimization problems. To strengthen the simulation results in reference 1, we apply the profile optimization method to two cases of airfoil shape optimization in transonic viscous flow over a range of Mach numbers.

The first case is the redesign of the RAE2822 airfoil (ref. 2) over the Mach range from 0.68 to 0.76, with the target lift at 0.733 and Reynolds number 2.7×10^6. The second case is the redesign of Whitcomb's integral supercritical airfoil (ref. 3) over the Mach range from 0.68 to 0.77, with the target lift at 0.7 and Reynolds number 2.7×10^6. Viscous flow analysis and the corresponding gradient calculation are based on FUN2D (ref. 4), which can perform fully turbulent Navier-Stokes flow analysis and the corresponding discrete adjoint analysis with unstructured grids. Two spar location thickness constraints and the maximum thickness constraint are enforced for both airfoil shape optimization cases. Airfoils are parameterized by 35 B-spline control points. Design variables are angles of attack at specified design conditions and the y-coordinates of 35 B-spline control points.

In both cases, the simulation results show that the profile optimization method can generate fairly realistic optimal airfoil shapes in transonic viscous flow without severe off-design performance degradation, when 4 design conditions and 35 geometric design variables are used.

Because the purpose of this paper is to provide additional simulation results for the profile optimization method given in reference 1, readers should consult reference 1 for relevant references and technical details.

The paper is organized as follows. In section 2, we review the profile optimization method. Section 3 includes the simulation results for airfoil shape optimization in transonic viscous flow. Concluding remarks are given in the final section.

2 Profile Optimization Method

In this section, we briefly review the profile optimization method proposed in reference 1. The profile optimization method is intended to solve the following robust optimization problem:

$$\min_{D,\alpha(M)} \Big(E(c_d), \sigma(c_d) \Big) \tag{1}$$

subject to

$$D \in \mathcal{F} \quad \text{and} \quad c_l(D, \alpha(M), M) = c_l^*(M) \quad \text{for } M \in \Omega. \tag{2}$$

Here $c_l^*(M)$ is the target lift requirement for Mach number M, $\mathcal{F}$ is a given feasible set for geometric design variables (that could be defined by geometry constraints such as thickness constraints), and $\alpha(M)$ is the angle of attack corresponding to M. The drag and lift coefficients are c_d and c_l, respectively. The mean and variance of c_d are defined as

$$\left.\begin{aligned} E(c_d) &= \int_\Omega c_d(D, \alpha(M), M) \cdot p(M)\, dM, \\ \sigma^2(c_d) &= \int_\Omega \left[c_d(D, \alpha(M), M) - E(c_d) \right]^2 p(M)\, dM, \end{aligned}\right\} \tag{3}$$

where $p(M)$ is a probability density function of M and Ω is a given Mach range (such as from $M = 0.68$ to $M = 0.77$).

The robust optimization model in equation (1) addresses some important issues in aerodynamic shape optimization. For example, to avoid off-design performance degradation, one can reduce $\sigma(c_d)$ as much as possible. Note that if $\sigma(c_d) = 0$, the corresponding solution will

have the same (perhaps poor) performance over the given Mach range. Therefore, equation (1) provides a tool for trade-offs between average performance improvement and performance fluctuations over the Mach range. However, due to the high computational cost for solving Navier-Stokes equations, it is impossible to have reasonable estimates of $E(c_d)$ and $\sigma(c_d)$. Consequently, it is not practical to solve equation (1) using current computational fluid dynamics tools.

One alternative way to avoid off-design performance degradation is to find a descent direction that could reduce the drag *simultaneously* and *proportionally* over the given Mach range while keeping the lift at the target value. The profile optimization method was designed to find such a descent direction with limited information on lift and drag over the given Mach range. The innovative feature of the profile optimization method is to adaptively change the objective function from iteration to iteration to achieve simultaneous and proportional drag reduction over the given Mach range. In contrast to methods that minimize one aggregate objective function to find a Pareto optimal solution to a multiobjective optimization problem, the profile optimization method does not solve any optimization problem with one objective function; instead, it looks for a Pareto optimal solution that has the least chance for severe off-design performance degradation.

Profile Optimization Method. Let D^0 be a given initial design vector, let $M_1, \ldots, M_r$ be a set of design points over the given Mach range, and $k = 0$. Construct a sequence of design vectors as follows:

1. Compute feasible angles of attack. Find $\alpha_{1,k}, \alpha_{2,k}, \ldots, \alpha_{r,k}$ such that
$$c_l(D^k, \alpha_{i,k}, M_i) = c^*_{l,i} \quad \text{for } 1 \le i \le r.$$

2. Solve a trust region subproblem. Let $c_{d,i,k}$ and $c_{l,i,k}$ be the linear approximations of the drag and lift at $(D^k, \alpha_{i,k})$:
$$c_{l,i,k}(\Delta D, \Delta\alpha_i) = c_l(D^k, \alpha_{i,k}, M_i) + \left\langle \frac{\partial c_l}{\partial D}, \Delta D \right\rangle + \frac{\partial c_l}{\partial \alpha}\Delta\alpha_i,$$
$$c_{d,i,k}(\Delta D, \Delta\alpha_i) = c_d(D^k, \alpha_{i,k}, M_i) + \left\langle \frac{\partial c_d}{\partial D}, \Delta D \right\rangle + \frac{\partial c_d}{\partial \alpha}\Delta\alpha_i,$$
where the derivatives are evaluated at $(D^k, \alpha_{i,k}, M_i)$. Consider the following trust region subproblem:
$$\min_{\Delta D, \Delta\alpha_i} \quad \eta \qquad \text{subject to} \quad D^k + \Delta D \in \mathcal{F}, \tag{4}$$
$$-\delta_{i,k}\rho_k \le \Delta D_i \le \delta_{i,k}\rho_k \quad \text{for } 1 \le i \le n,$$
$$-\alpha_k \le \Delta\alpha_i \le \alpha_k \quad \text{for } 1 \le i \le r,$$
$$c_{l,i,k}(\Delta D, \Delta\alpha_i) = c^*_{l,i} \quad \text{for } 1 \le i \le r,$$
$$c_{d,i,k}(\Delta D, \Delta\alpha_i) \le (1-\eta)\cdot c_d(D^k, \alpha_{i,k}, M_i) \quad \text{for } 1 \le i \le r,$$
where $\delta_{i,k} \ge 0$ and $\alpha_k > 0$ are scalars that determine the trust region, and $D^k + \Delta D \in \mathcal{F}$ means that the airfoil corresponding to $(D^k + \Delta D)$ satisfies all the geometric constraints. (For our simulation runs, $\delta_{i,k}$ is approximately the thickness of the airfoil at the x-coordinate of the ith control point, $\alpha_k = 1$, and $D^k + \Delta D \in \mathcal{F}$ means that the airfoil satisfies two thickness constraints at the spar locations and the maximum thickness constraint.) Determine the smallest $\rho_k > 0$ such that equation (4) is feasible and the least norm solution $(\Delta D^k, \Delta\alpha_{1,k}, \ldots, \Delta\alpha_{r,k})$ of equation (4) satisfies the following condition:
$$c_{d,i,k}(\Delta D^k, \Delta\alpha_{i,k}) \le (1-\gamma_{\min})c_d(D^k, \alpha_{i,k}, M_i) \quad \text{for } 1 \le i \le r.$$

3. Generate the new iterate. Let $\alpha_{i,k+1} = \alpha_{i,k} + \Delta\alpha_{i,k}$ for $1 \leq i \leq r$ and $D^{k+1} = D^k + \Delta D^k$.

4. Start a new iteration. Update k by $k+1$ and go back to step 1.

3 Numerical Simulation Results

We apply the profile optimization method in two cases of airfoil shape design optimization in transonic viscous flow. The first case is the redesign of the RAE2822 airfoil over the Mach range from 0.68 to 0.76. We adopt the four design conditions used in Drela's simulation (ref. 2): $M = 0.68, 0.71, 0.74$, and 0.76, with the target lift at 0.733 and Reynolds number 2.7×10^6. The second case is the redesign of Whitcomb's integral supercritical airfoil (ref. 3) over the Mach range from 0.68 to 0.77. In this case, we use the following four design conditions: $M = 0.68, 0.71, 0.74$, and 0.77, with the target lift at 0.7 and Reynolds number 2.7×10^6.

For a given airfoil, the lift and drag coefficients and their gradients are calculated by solving fully turbulent Navier-Stokes equations and the corresponding discrete adjoint equations using FUN2D (ref. 4). In both cases, the unstructured grid has 300 grid points on the airfoil and 32 grid points on the far field (which is placed at 20 chord lengths). The unstructured grid has a total of 18654 grid points, 55631 elements, and 37308 faces (see fig. 1 for the grid near the RAE2822 airfoil).

With the given grid, the flow solver and the adjoint solver are terminated when the 2-norms of the residual of the density equations and the corresponding discrete adjoint equations are reduced by at least five orders of magnitude.

Airfoils are parameterized by 35 B-spline control points, which is large enough to accommodate free-form geometry changes for both cases. Figure 2 shows parameterization of the RAE2822 airfoil and Whitcomb's integral supercritical airfoil.

The x-coordinates of all the control points are fixed during optimization. Changes of the y-coordinates of the five control points near the trailing edge are constrained to be the same so that the shape of the airfoil near the trailing edge is not too oscillatory. The same geometry constraint is applied to the y-coordinates of the three control points near the leading edge. The reason for such geometric constraints is that the optimizer may not be able to make a reasonable modification of the shape of the leading or trailing edge at very fine scales. All the y-coordinates of the 35 control points are used as shape design variables. In both cases, we impose a thickness constraint at spar locations $x/c = 0.15$ and $x/c = 0.6$ and at the maximum thickness location. For each iterate D^k, we find angles of attack $\alpha_{1,k}, \ldots, \alpha_{r,k}$ such that $|c_l(D^k, \alpha_{i,k}, M_i) - c^*_{l,i}|/c^*_{l,i} \leq 0.001$.

3.1 Drag Reduction Over the Given Mach Range

Figures 3 and 4 show the history of drag changes at the design conditions for cases 1 and 2, respectively.

Figure 5 shows the postoptimization analysis of drag curve over the given Mach range for cases 1 and 2. The drag rise curves are constructed by using 10 equally spaced Mach numbers from $M = 0.68$ to $M = 0.77$, which include 4 design points and 6 off-design points. In both cases, the profile optimization method reduces the drag of the baseline over the given Mach range. Moreover, there is no off-design performance degradation of the optimized airfoils.

3.2 Airfoil Shapes

The optimal airfoils generated by the profile optimization method are quite smooth and do not have shock bumps corresponding to design conditions (i.e., Mach numbers). This result is different from the numerical simulation results obtained earlier by Drela (ref. 2) on multipoint airfoil optimization when sinusoidal basis functions were used to parameterize the airfoil shape. Figure 6 shows the optimal airfoils generated by the profile optimization method for cases 1 and 2.

3.3 Pressure Distributions

Pressure distributions for the baseline and the optimal airfoil in both cases are plotted in figures 7 and 8.

4 Concluding Remarks

This paper documents two cases of using the profile optimization method to redesign airfoils over a range of Mach numbers in transonic viscous flow with airfoils parameterized by 35 B-spline control points. FUN2D (ref. 4) is used to compute the lift and drag values and their gradients with respect to changes in airfoil shape and changes in angle of attack. All the y-coordinates of 35 B-spline control points are used by the profile optimization method to search for the true optimal solution. With thickness constraints at two spar locations and the maximum thickness constraint, the profile optimization method minimizes the drag at four design conditions while keeping the lift at the target value. The optimized airfoils have fairly realistic and smooth shapes. Postoptimization analysis shows that the optimized airfoils have no off-design performance degradation.

The simulation results demonstrate that the profile optimization method has the potential to be used for real-world airfoil shape optimization over a range of flight conditions.

References

[1] Li, W.; Huyse, L.; and Padula, S.: Robust Airfoil Optimization to Achieve Drag Reduction Over a Range of Mach Numbers, *Struc. Optim.*, vol. 24, no. 1, 2001, pp. 38–50.

[2] Drela, M.: Pros and Cons of Airfoil Optimization. *Frontiers of Computational Fluid Dynamics 1998*, D. A. Caughey and M. M. Hafez, eds., World Scientific, 1998.

[3] Harris, C.: *NASA Supercritical Airfoils – A Matrix of Family-Related Airfoils.* NASA/TP-1990-2969, 1990.

[4] Nielsen, E.: *FUN2D/3D: Fully Unstructured Navier-Stokes.* http://fun3d.larc.nasa.gov Accessed Apr. 18, 2003.

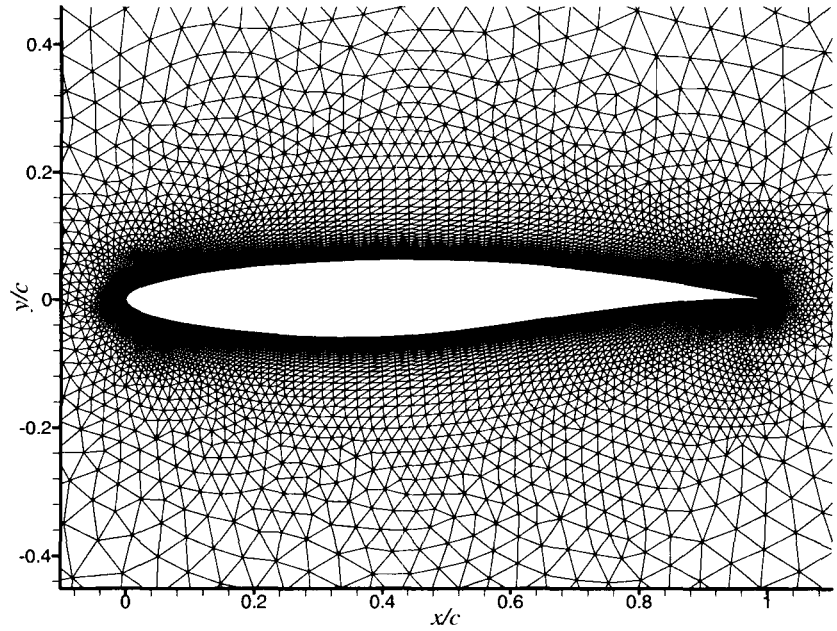

Figure 1: Grid used to solve Navier-Stokes equations by FUN2D.

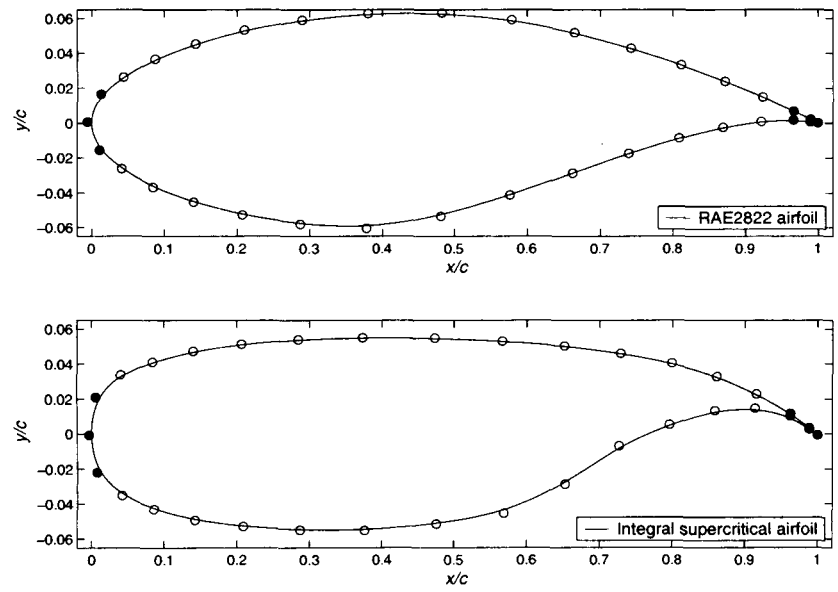

Figure 2: RAE2822 airfoil and Whitcomb's integral supercritical airfoil parameterized by 35 cubic B-spline control points.

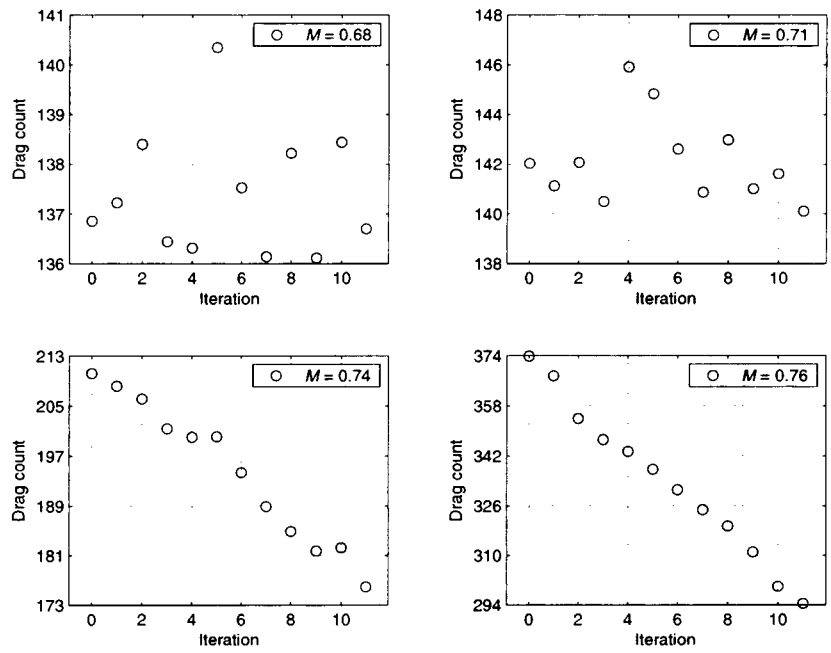

Figure 3: Changes of drag counts at four design conditions for case 1 with target lift 0.733.

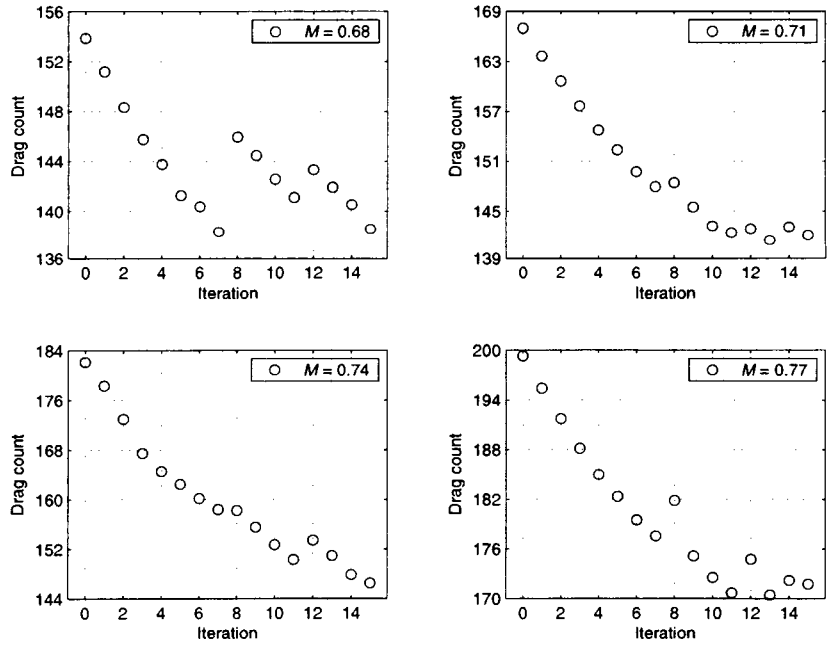

Figure 4: Changes of drag counts at four design conditions for case 2 with target lift 0.7.

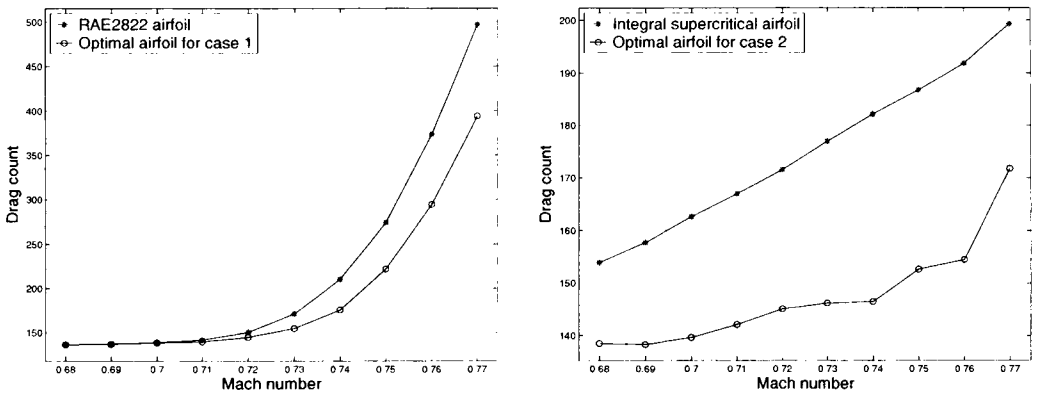

Figure 5: Postoptimization analysis of drag over given Mach range for case 1 with target lift 0.733 and case 2 with target lift 0.7.

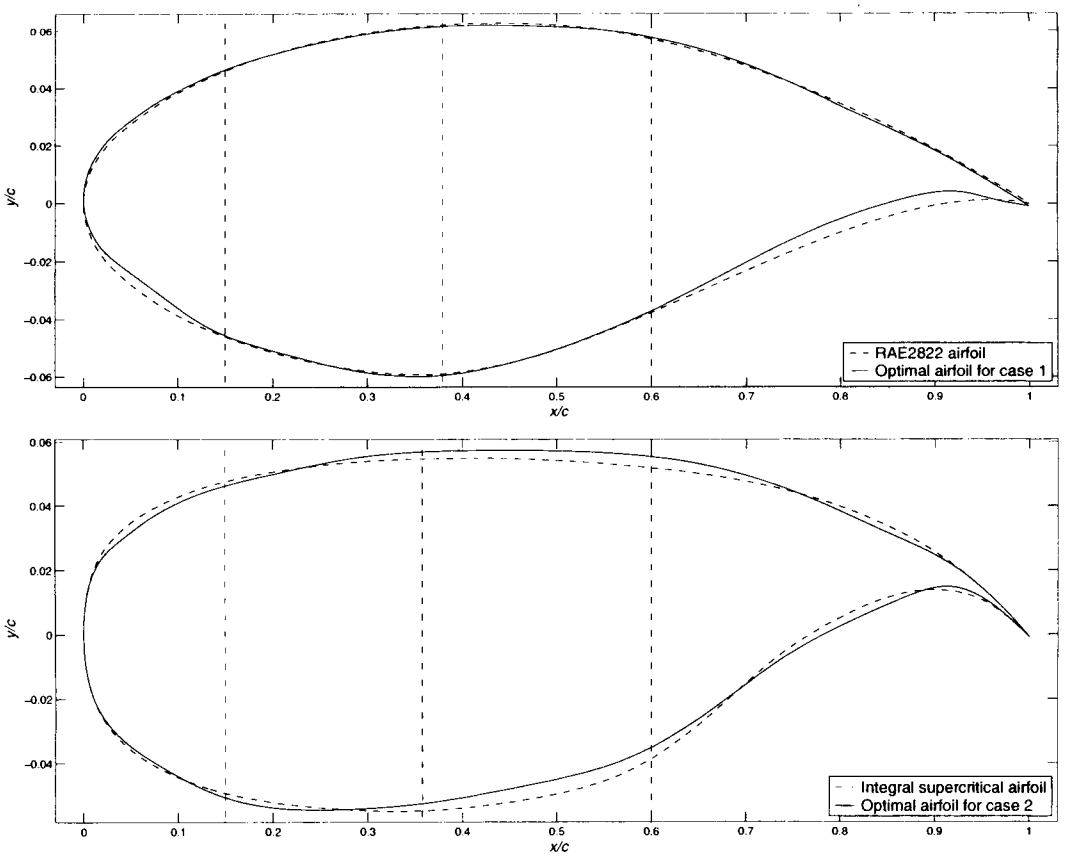

Figure 6: Optimal airfoils generated by profile optimization method.

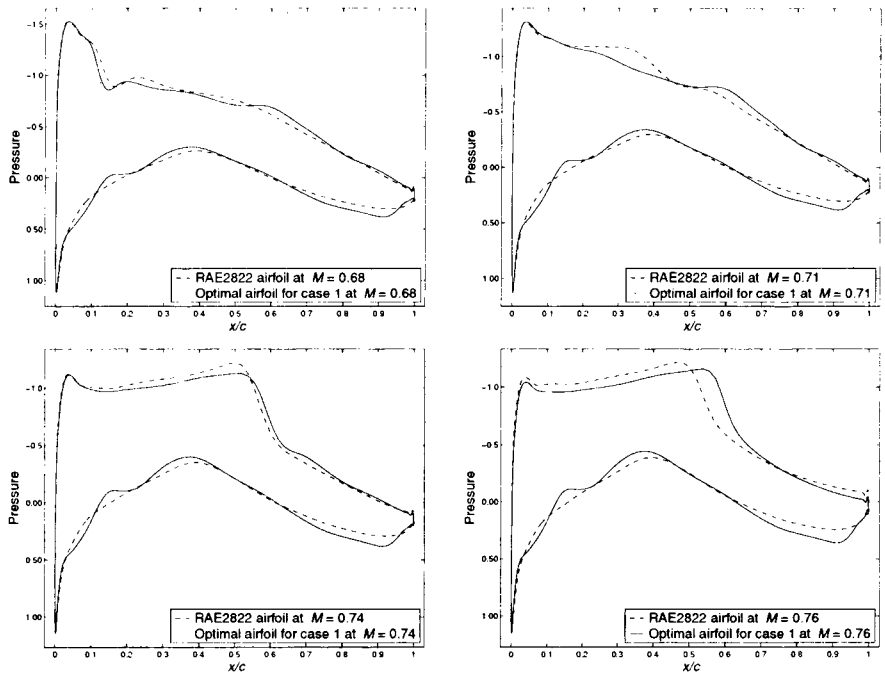

Figure 7: Pressure distributions on RAE2822 and the corresponding optimal airfoil at four design conditions with target lift at 0.733.

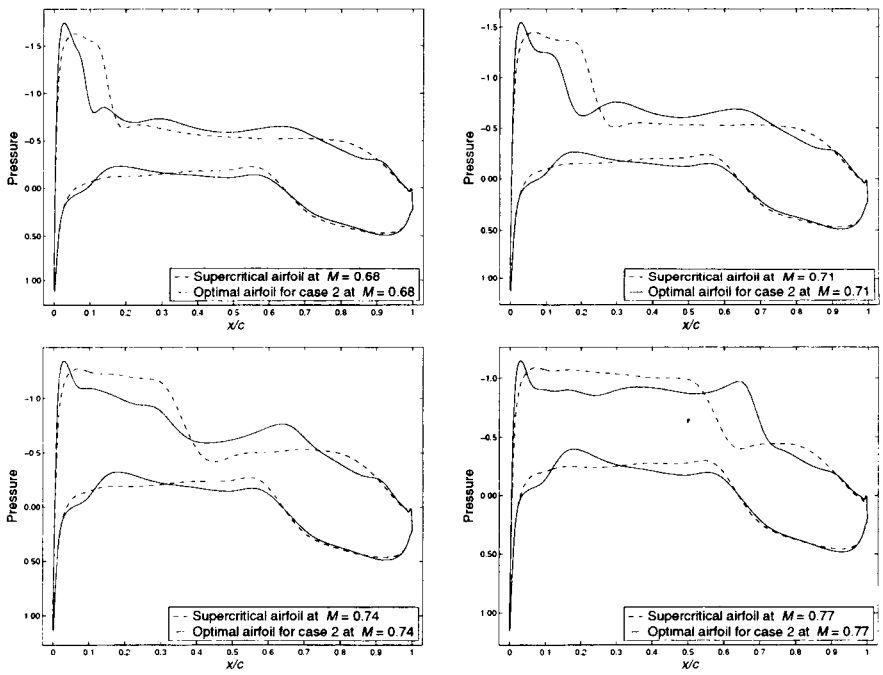

Figure 8: Pressure distributions on Whitcomb's integral supercritical airfoil and the corresponding optimal airfoil at four design conditions with target lift at 0.7.

REPORT DOCUMENTATION PAGE

Form Approved
OMB No. 0704–0188

1. REPORT DATE *(DD-MM-YYYY)*	2. REPORT TYPE	3. DATES COVERED *(From - To)*
01-05-2003	Technical Memorandum	

4. TITLE AND SUBTITLE
Profile Optimization Method for Robust Airfoil Shape Optimization in Viscous Flow

5a. CONTRACT NUMBER

5b. GRANT NUMBER

5c. PROGRAM ELEMENT NUMBER

6. AUTHOR(S)
Wu Li

5d. PROJECT NUMBER

5e. TASK NUMBER

5f. WORK UNIT NUMBER
762-20-61-01

7. PERFORMING ORGANIZATION NAME(S) AND ADDRESS(ES)
NASA Langley Research Center
Hampton, VA 23681-2199

8. PERFORMING ORGANIZATION REPORT NUMBER
L–18283

9. SPONSORING/MONITORING AGENCY NAME(S) AND ADDRESS(ES)
National Aeronautics and Space Administration
Washington, DC 20546-0001

10. SPONSOR/MONITOR'S ACRONYM(S)
NASA

11. SPONSOR/MONITOR'S REPORT NUMBER(S)
NASA/TM–2003–212408

12. DISTRIBUTION/AVAILABILITY STATEMENT
Unclassified-Unlimited
Subject Category 59
Availability: NASA CASI (301) 621-0390 Distribution: Standard

13. SUPPLEMENTARY NOTES
An electronic version can be found at http://techreports.larc.nasa.gov/ltrs/ or http://techreports.larc.nasa.gov/cgi-bin/NTRS.

14. ABSTRACT
Simulation results obtained by using FUN2D for robust airfoil shape optimization in transonic viscous flow are included to show the potential of the profile optimization method for generating fairly smooth optimal airfoils with no off-design performance degradation.

15. SUBJECT TERMS
robust optimization, airfoil shape optimization, multiobjective optimization, lift-constrained drag minimization, B-spline parameterization of airfoil

16. SECURITY CLASSIFICATION OF:			17. LIMITATION OF ABSTRACT	18. NUMBER OF PAGES	19a. NAME OF RESPONSIBLE PERSON
a. REPORT	b. ABSTRACT	c. THIS PAGE			STI Help Desk (email: help@sti.nasa.gov)
U	U	U	UU	14	19b. TELEPHONE NUMBER *(Include area code)* (301) 621-0390